Characterization and *in vitro* evaluation of biphasic calcium pyrophosphate–tricalciumphosphate radio frequency magnetron sputter coatings

K. Takahashi,[1] J.J.J.P. van den Beucken,[2] J.G.C. Wolke,[2] T. Hayakawa,[3] N. Nishiyama,[3] J.A. Jansen[2]
[1]*Department of Dental Materials, Nihon University Graduate School of Dentistry at Matsudo, 2-870-1, Sakaecho Nishi, Matsudo, Chiba 271-8587, Japan*
[2]*Department of Periodontology and Biomaterials, Radboud University Nijmegen Medical Center, P.O. Box 9101, 6500 HB Nijmegen, The Netherlands*
[3]*Department of Dental Biomaterials, Research Institute of Oral Science, Nihon University School of Dentistry at Matsudo, 2-870-1, Sakaecho Nishi, Matsudo, Chiba 271-8587, Japan*

Received 11 December 2006; revised 26 January 2007; accepted 31 January 2007
Published online 16 July 2007 in Wiley InterScience (www.interscience.wiley.com). DOI: 10.1002/jbm.a.31341

Abstract: The objective of this study was to characterize the physicochemical, dissolution, and osteogenic properties of radio frequency magnetron sputtered dicalcium pyrophosphate/tricalciumphosphate (Pyro/TCP) and hydroxylapatite (HA) coatings. Therefore Pyro/TCP and HA coatings were deposited on grit-blasted titanium discs. The results showed that the deposited coatings were amorphous and changed into a crystalline structure after IR heat-treatment of 550°C for HA and 650°C for Pyro/TCP. Heat-treated HA coatings appeared to be stable during immersion in simulated body fluid (SBF), that is no changes in the XRD pattern were observed. Also, no dissolution of the coating was observed by scanning electron microscopy (SEM). Energy dispersive spectroscopy (EDS) revealed that the Ca/P ratio of the HA coatings remained constant during SBF immersion. On the other hand, the heat-treated Pyro/TCP coatings showed a surface reaction of calcium pyrophosphate into a β-tricalcium phosphate phase during SBF immersion. This was confirmed by EDS analysis. Rat bone marrow-derived osteoblast-like cells cultured on the heat-treated substrates showed that cell proliferation and differentiation occurred on both types of bioceramic coatings. No significant differences for proliferation and early differentiation were observed between cells cultured on heat-treated Pyro/TCP and HA at individual time points. However, osteocalcin expression, a late marker for osteoblast-like cell differentiation, was significantly increased after 12 days of culture on HA-coatings. These results were confirmed by SEM observations and suggest increased osteogenic properties for HA-coatings over Pyro/TCP-coatings. Additional research is necessary to obtain conclusive evidence on the *in vivo* osteogenic capacity of Pyro/TCP coatings. © 2007 Wiley Periodicals, Inc. J Biomed Mater Res 84A: 682–690, 2008

Key words: RF magnetron sputter coatings; biphasic; pyrophosphate; tricalciumphosphate; osteoblast-like cell

INTRODUCTION

Calcium phosphate (CaP) coatings have been used for medical and dental implants because of their superior bone biocompatibility and osteointegrative properties.[1] Various coating techniques are available for the deposition of calcium phosphate on titanium implants, such as plasma-spray technique,[2] ion plating,[3] radio frequency (RF) magnetron sputtering,[4] ion beam dynamic mixing,[5] and electrostatic spray deposition.[6–8] RF magnetron sputtering deposition has some clear advantages compared to other CaP deposition techniques. These advantages include the production of stable, dense, adherent, and homogeneous thin Ca-P coatings on a metal substrate.[9] Frequently, these coatings have an amorphous structure directly after deposition, which can easily be transformed into crystalline phases by rapid heat treatment with, for example, infrared radiation.[10] Recently, a lot of attention has been paid to pyrophosphate (Pyro) ceramics. As an intermediate product in the biological mineralization process, Pyro has been demonstrated to have great potential as an *in vivo* biodegradable bone substitute.[11] Synthetic Pyro can inhibit osteoclastic bone resorption, and therefore is used for the treatment of bone diseases including tumor-induced hypercalcemia and osteoporosis.[12,13] Previous studies in our laboratory demonstrated that Pyro can also be applied as a coating on titanium using RF magnetron sputtering.[4]

Correspondence to: J.A. Jansen; e-mail: j.jansen@dent.umcn.nl

The dissolution behavior in simulated body fluid of RF magnetron sputtered Pyro coatings was similar as compared to HA coatings. Further, rat bone marrow osteoblast-like cells proliferated only on crystalline magnetron sputtered Pyro and HA coatings, during which crystalline HA coatings induced an earlier osteogenic effect than crystalline Pyro coatings.[14–17] Different approaches are applied to improve the osteogenic capacity of biomaterials. Among them, the use of osteogenic cells and adding growth factors are common approaches. Further, modification of the physicochemical properties of an implant material, like composition, crystallinity, and macro- and microporosity, is another potential method to improve the osteogenic capacity.[18] For example, porous hydroxylapatite ceramic was shown to be less osteoconductive than a biphasic calcium phosphate (BCP).[17] Also, other studies confirmed that BCP ceramics, composed of a mixture of HA and β-tricalciumphosphate (β-TCP), induce increased bone formation when implanted compared to pure HA ceramic.[19–21]

In view of the above mentioned, the objective of this study was to characterize the physicochemical and dissolution behavior of Pyro/β-TCP and HA coatings obtained by RF magnetron sputtering as well as their effect on the behavior of osteoblast-like cells.

MATERIALS AND METHODS

Materials

For the experiments, titanium substrates with a diameter of 12 mm and thickness of 2 mm were used. All the discs were Al_2O_3 grit-blasted at one side (Ra = 1.0–1.3 μm) prior to coating deposition. RF magnetron sputter deposition was performed using an Edwards High Vacuum ESM 100 sputter system. The target materials used for the deposition were either a mixture of 50% Pyro (β-$Ca_2P_2O_7$)/50% β-TCP ($Ca_3(PO_4)_2$) or HA ($Ca_5(PO_4)_5OH$) granulate.

RF magnetron sputtering

The substrates were mounted on a rotating and water-cooled substrate holder. The distance between target and substrate was 80 mm. Before sputtering the metal substrates were cleaned by etching for 10 min with argon ions. During deposition, argon pressure was kept at 5×10^{-3} mbar. Pyro/TCP and HA coatings were prepared at a discharge power of 400 W with coating thickness of 2 μm. After deposition, the as-coated specimens were subjected to an additional infrared heat treatment for 30 s, for which the settings were based on previous experiments[4]; the Pyro/TCP coatings at 650°C and the HA coatings at 550°C (Quad Ellipse Chamber, Model E4-10-P, Research).

Characterization of the coatings

As-deposited coatings and heat-treated coatings were characterized using the following techniques:

X-ray diffraction

The crystallographic structure of each coating was determined by thin film X-ray diffraction (XRD) using a Philips θ-2θ diffractometer (PW 3710, 40 kV, 40 mA) using a CuKα-radiation of 1.5418 Å wavelength. For these measurements, the specimens were scanned from 20–39° (2θ) at a scanning speed of 0.008°/s and a stepsize of 0.01° (2θ).

Fourier transform infrared spectroscopy

The infrared spectra of the coatings on the substrates were obtained by reflection Fourier transform infrared spectroscopy (FTIR) (Spectrum One, Perkin-Elmer), since infrared radiation cannot pass through the titanium substrate. The coatings were analyzed in the range of 4000–400 cm^{-1} at 2 cm^{-1} resolution and 16 scans. All spectra were recorded at ambient temperature.

Scanning electron microscopy

The surface morphology of the coatings was examined using SEM using a Jeol 6310 SEM at an accelerating voltage of 10 kV after Au coating.

Energy dispersive spectroscopy

The above described scanning electron microscope was equipped with an energy-dispersive X-ray microanalyzer (Voyager). Energy dispersive spectroscopy (EDS) was carried out at a magnification of 500× at an accelerating voltage of 10 kV to determine the elemental composition of deposited coatings. Stochiometric hydroxylapatite discs of known Ca/P ratio and of equal thickness to the coated Ti-substrates (1.5 mm) were used as a reference for the determination of Ca/P ratios of the deposited Ca/P coatings.

In vitro bioactivity assay

Specimens (heat-treated) were immersed in 4 mL simulated body fluid (SBF) with a pH of 7.2 at 37°C (Table I).[22] At time points 1, 2, 3, and 4 weeks, the SBF buffer solution was refreshed. The specimens were retrieved out of the SBF solution, thoroughly rinsed in milliQ, and dried at room temperature. Subsequently, the specimens were characterized using XRD, FTIR, SEM, and EDS, as described previously.

TABLE I
Concentrations of Ionic Species (m*M*) in Simulated Body Fluid (SBF) and Human Blood Plasma (HBP)

Ions	Na	K	Ca	Mg	Cl	CO_3	PO_4	SO_4
SBF	142	5	2.5	1.5	148	4.2	1	0.5
HBF	142	5	2.5	1.5	103	27	1	0.5

Cell culture experiment

Isolation of rat bone marrow cells

Cells were isolated and cultured using the method described by Maniatopoulos et al.[23] Briefly, bone marrow cells were obtained from femora of male Wistar rats. Femora were washed four times in α-MEM (Gibco) with 0.5 mg/mL gentamycin and 3 μg/mL fungizone. Epiphyses were cut off and diaphyses flushed out with 15 mL α-MEM, supplemented with 10% fetal calf serum (FCS), 50 μg/mL ascorbic acid, 50 μg/mL gentamycin, 10 m*M* Na β-glycerophosphate, and 10^{-8}*M* dexamethasone. Cells were incubated in a humidified atmosphere (95% air; 5% CO_2; 37°C). The medium was changed three times a week. After 7 days of primary culture, cells were detached using 0.25% w/v trypsin and counted using a Coulter® counter. Experimental substrates were placed at the bottom of 24-well plates, and 1 mL cell suspension (4.0×10^4 cells/mL) was added to the substrates. Medium was refreshed three times a week.

Proliferation assay

To determine cellular proliferation, cellular protein concentrations were measured with a micro BCA (bicinchoninic acid) protein assay (Pierce). After 4, 8, 12, and 16 days, experimental substrates were washed twice with PBS and immersed in milliQ. Subsequently, three repetitive freeze/thaw cycles were carried out prior to the assay. For the assay, 100 μL of sample was incubated with 100 μL working solution for 2 h at 37°C. Serial dilutions of BSA (2–200 μg/mL) were used for standard curve. The plate was read at 570 nm in an ELISA plate reader (Bio-Tek). A total of three independent runs were performed, in which at each time point, four substrates per condition were used ($n = 4$).

Differentiation assay

To determine cell differentiation, alkaline phosphatase (ALP) activity was measured at 4, 8, 12, and 16 days using the same samples as those from the proliferation assay. Eighty microliters of sample and 20 μL of alkaline buffer (Sigma, Zwijndrecht, The Netherlands) were added to 100 μL of substrate solution (5 m*M* paranitrophenylphosphate: Sigma). For the standard curve, serial dilutions of 4-nitrophenol (0–25 nmol/mL) were made. The plate was incubated at 37°C for 60 min. The reaction was stopped by the addition of 100 μL of 0.3*M* NaOH, after which the plate was read in an ELISA reader (Bio-Tek, USA). A total of three independent runs were performed, in which at each time point, four substrates per condition were used ($n = 4$). Measurements were then normalized for protein assay.

Osteocalcin assay

Osteocalcin (OC) was measured in the cell cultures by enzyme immunoassay (EIA; Biomedical Technologies). After 8, 12, 16, and 24 days of culture, samples were collected by scraping in EIA sample buffer and sonicated for 10 min. About 100 μL of sample was added to the wells and the plate was incubated at 4°C for 18 h. The plate was washed three times, 100 μL of antiserum was added, and the plate was incubated for 1 h at 37°C. After washing three times, 100 μL of donkey anti-goat IgG peroxidase was added and incubated for 1 h at room temperature. The plate was washed, 100 μL of substrate solution (1 volume TMB ($3,3^1,5,5^1$)-tetramethylbenzidine)/1 volume H_2O_2) was added, and the plate was incubated for 30 min. Then 100 μL stop solution was added and the plate was read at 450 nm in an ELISA plate reader. A total of three independent runs were performed, in which at each time point, four substrates per condition were used ($n = 4$).

Cell morphology

Samples with cells for SEM were fixed in 2% glutaraldehyde, washed twice in 0.1*M* sodium-cacodylate buffer (pH 7.4), and dehydrated using a graded series of ethanol. After drying with tetramethylsilane, samples were sputter-coated with gold and examined using a Jeol 6310 SEM with an acceleration voltage of 15 kV.

Statistical analysis

The entire cell culture experiment was preformed three times, and for each cell culture run cells were isolated from one individual rat. Differences between experimental groups were calculated using an ANOVA followed by a Student-Newman-Keuls test. Calculations were performed in GraphPad Instat, Version 3.05 (GraphPad Software, San Diego, CA).

RESULTS

Coating characterization before and after heat treatment

X-ray diffraction

The XRD patterns of the as-deposited coatings showed an amorphous structure with no clear reflection, only the underlying substrate peaks were visible (Fig. 1). Infrared heat-treatment at 550°C changed the amorphous sput-

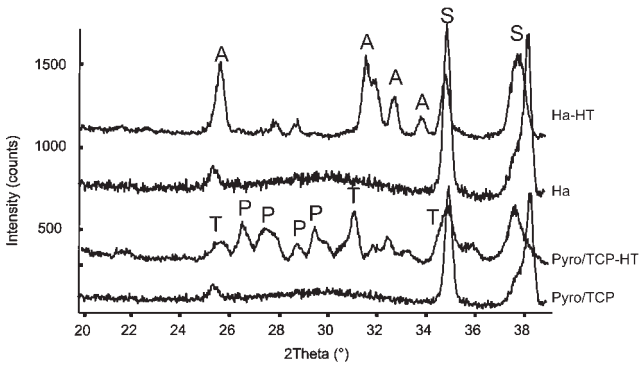

Figure 1. XRD patterns of sputtered Ca-P coatings. The major peaks have been marked: A, apatite; P, pyrophosphate; T, tri-calciumphosphate; S, substrate (titanium).

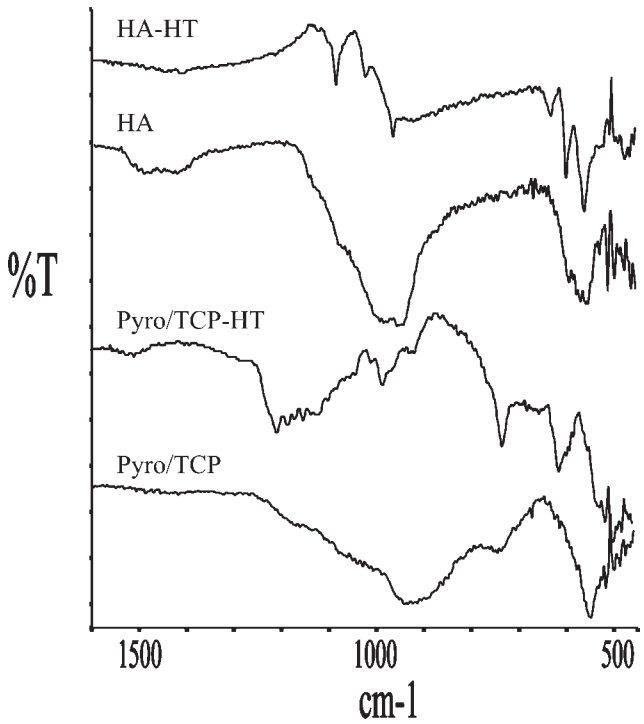

Figure 2. FTIR spectra of sputtered Ca-P coatings.

tered HA coating into a crystalline apatite structure with reflections 002, 211, 112, 202 at respectively 25.9°, 31.9°, 32.4° and 34.0° (2θ), comparative with the XRD pattern of HA powder (JCPDS No. 09-0432). The sputtered amorphous pyrophosphate/tricalciumphosphate coating required an annealing temperature of 650°C. The amorphous phase changed into two crystalline phases, a beta calcium pyrophosphate structure with peaks at 26.6°, 27.7°, 28.5° and 29.5° (2θ) and a β-tricalciumphosphate structure with peaks at 25.7°, 31.0° and 34.4° (2θ).

Fourier transform infrared spectroscopy

Figure 2 shows the FTIR spectra of the as-deposited and heat-treated Pyro/TCP and HA coatings. All as-deposited Pyro/TCP and HA coatings show two clusters of peaks from 900–1150 and from 550–600 cm^{-1}, which can be attributed to the major absorption modes of phosphate bonds (Fig. 2). Infrared heat treatment of the HA coatings resulted in the appearance of various P—O bonds at a wavelength around 567, 587, 1009, and 1083 cm^{-1}, characteristic for apatite. The spectrum of the heat-treated Pyro/TCP coating revealed characteristics of a mixture of β-calcium pyrophosphate and β-tricalcium phosphate phases with various P—O bands at wavelengths of 523, 587, 612, 648, 970, 998, 1081, 1102, 1124, 1152, and 1203 cm^{-1}.

Scanning electron microscopy

SEM examination of the sputtered coatings showed an excellent coverage of the substrate surface. Infrared heat treatment had no effect on the coating morphology [Fig. 3(a-d)].

Energy dispersive spectroscopy

EDS analysis revealed that Ca/P ratios of amorphous as well as crystalline coatings was $\sim 1.43 \pm 0.03$ for Pyro/TCP, 1.97 ± 0.05 for HA (Table II).

In vitro bioactivity

X-ray diffraction

The XRD evaluation confirmed that the heat-treated Pyro/TCP and HA coatings were still present after 4 weeks of immersion in SBF [Fig. 4(a,b)]. The XRD patterns of the heat-treated Pyro/TCP and HA coatings did not change during incubation.

Fourier transform infrared spectroscopy

Figure 5(a,b) depicts the FTIR spectra of the SBF immersed coatings. Heat-treated Pyro/TCP and HA coatings showed stable FTIR spectra, almost no changes could be observed during 4 weeks of immersion in SBF.

Scanning electron microscopy

After immersion in SBF, SEM examination of the heat treated Pyro/TCP and HA coatings showed no change in morphology [Fig. 3(b-d)].

Energy dispersive spectroscopy

EDS examination showed that the Ca/P ratio of the HA coatings remained constant during SBF immersion, while the Pyro/TCP coatings changed from 1.43 to 1.70 after incubation in SBF (Table II).

Cell culture experiment

A total of three experimental runs were carried out, which showed similar results for proliferation, differentiation, and morphology. Below, results of one representative experimental run are presented.

Proliferation assay

The data are shown in Figure 6. For heat-treated coatings, protein content increased from day 4 to day 16 of culture at individual time points. No significant difference in protein content was observed between heat-treated Pyro/TCP and HA coatings ($p > 0.05$).

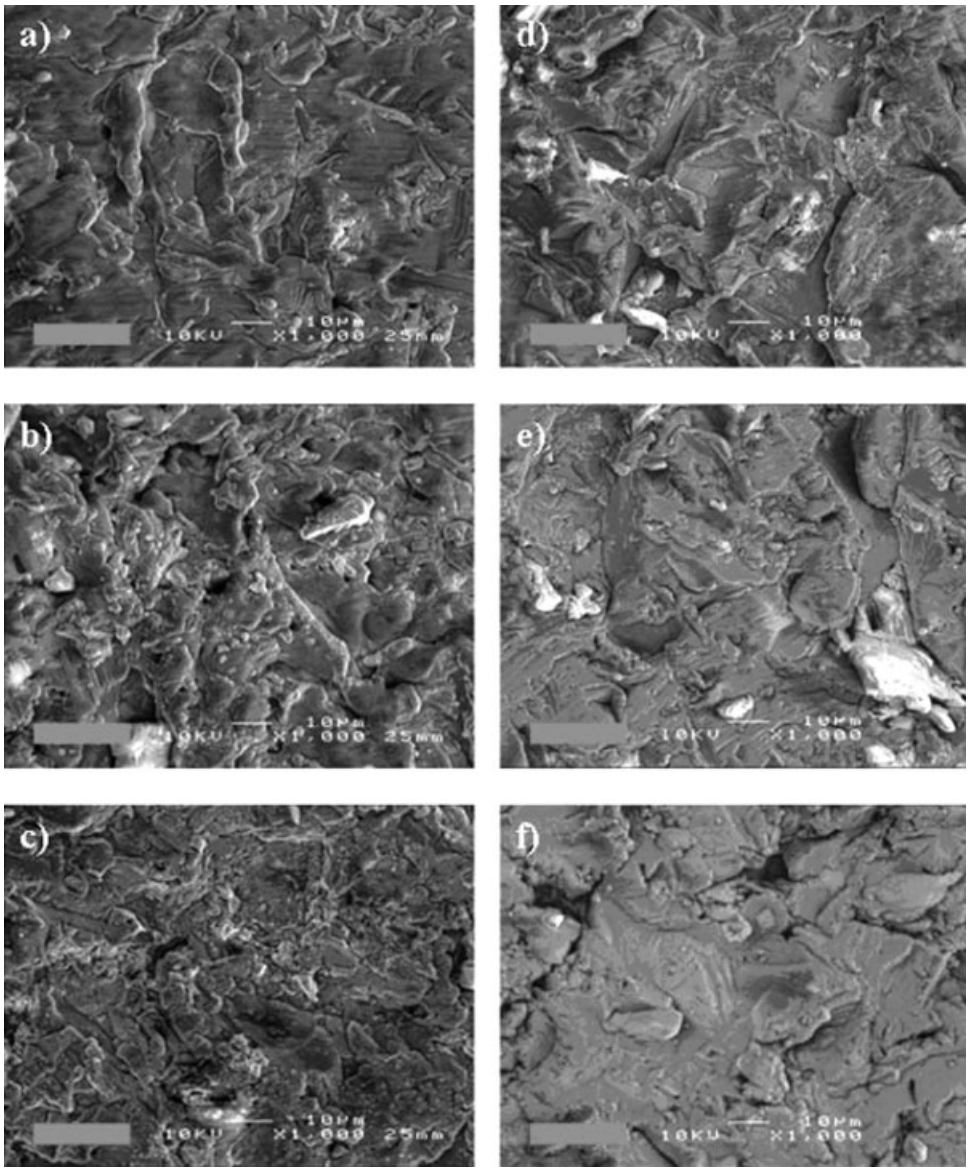

Figure 3. SEM pictures of coatings as-sputtered, heat-treated, and after incubation in SBF. (a–c) Pyro/TCP as-sputtered, and after 2 and 4 weeks SBF immersion; (d–f) HA as-sputtered, and after 2 and 4 weeks SBF immersion (Original magnification ×1000).

Alkaline phosphatase activity assay

The data are shown in Figure 7. ALP activity increased to a maximum on day 16 on Pyro/TCP coatings. For heat-treated HA coatings, ALP activity increased from day 4 and reached a maximum at day 8–12. No significant difference in ALP expression was observed between heat-treated Pyro/TCP and HA at individual time points ($p > 0.05$).

Osteocalcin assay

The data are shown in Figure 8. For both heat-treated coatings, OC expression increased from day 8

TABLE II
EDS Measurement of the Ca/P Ratio of the Heated Coatings Before and After Incubation in SBF

Week	Initial	1	2	3	4
Pyro/TCP	1.43 ± 0.03	1.56 ± 0.05	1.45 ± 0.10	1.70 ± 0.06	1.65 ± 0.03
HA	1.97 ± 0.05	1.98 ± 0.07	1.93 ± 0.09	2.01 ± 0.03	1.92 ± 0.03

Values are mean ± SD.

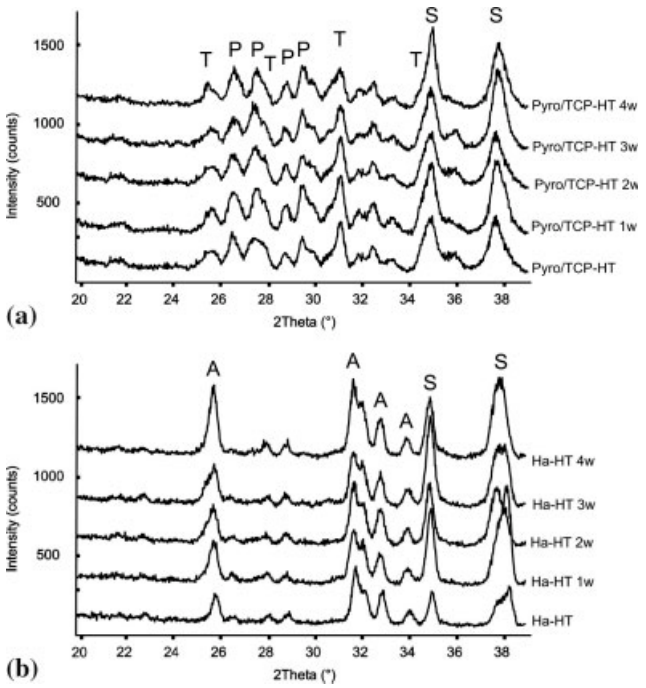

Figure 4. XRD patterns of sputtered Ca-P coatings after incubation in SBF; (a) pyro/TCP coatings (b) HA coatings.

to a maximum at day 16. After 12 days of culture, the OC expression on the heat treated HA coatings was significantly higher ($p < 0.01$) compared to the heat-treated Pyro/TCP coatings.

Cell morphology

After 8 days, cells started to form a multilayer on both Pyro/TCP and HA coatings. No apparent difference in cell morphology could be discerned between the two types of ceramic coating. After 24 days of culture, the cells had formed a layer of calcified globular accretions associated with collagen bundles. On the Pyro/TCP coatings, the cells had proliferated well and showed massive collagen fiber formation and surface mineralization in the form of globular accretions. On HA coatings, this process was observed to occur somewhat earlier (Fig. 9).

DISCUSSION

The purpose of this study was to characterize the physicochemical and dissolution behavior of Pyro/TCP and HA coatings obtained by RF magnetron sputtering. In addition, the *in vitro* cell behavior of RBM-osteoblast-like cells on RF magnetron Pyro/TCP and HA coatings was evaluated.

Physicochemical analysis demonstrated that as-deposited CaP coatings had an amorphous structure. The additional IR heat treatment induced crystal growth within the coatings, resulting in a crystalline structure. Heat treatment below 650°C did not crystallize the amorphous Pyro/TCP, while amorphous HA coatings transformed into a crystalline apatite structure at 550°C. However, after a heat-treatment at 650°C, the amorphous Pyro/TCP coatings changed into a crystalline β-Pyro/β-TCP structure. The main reason for the difference in crystallization can be

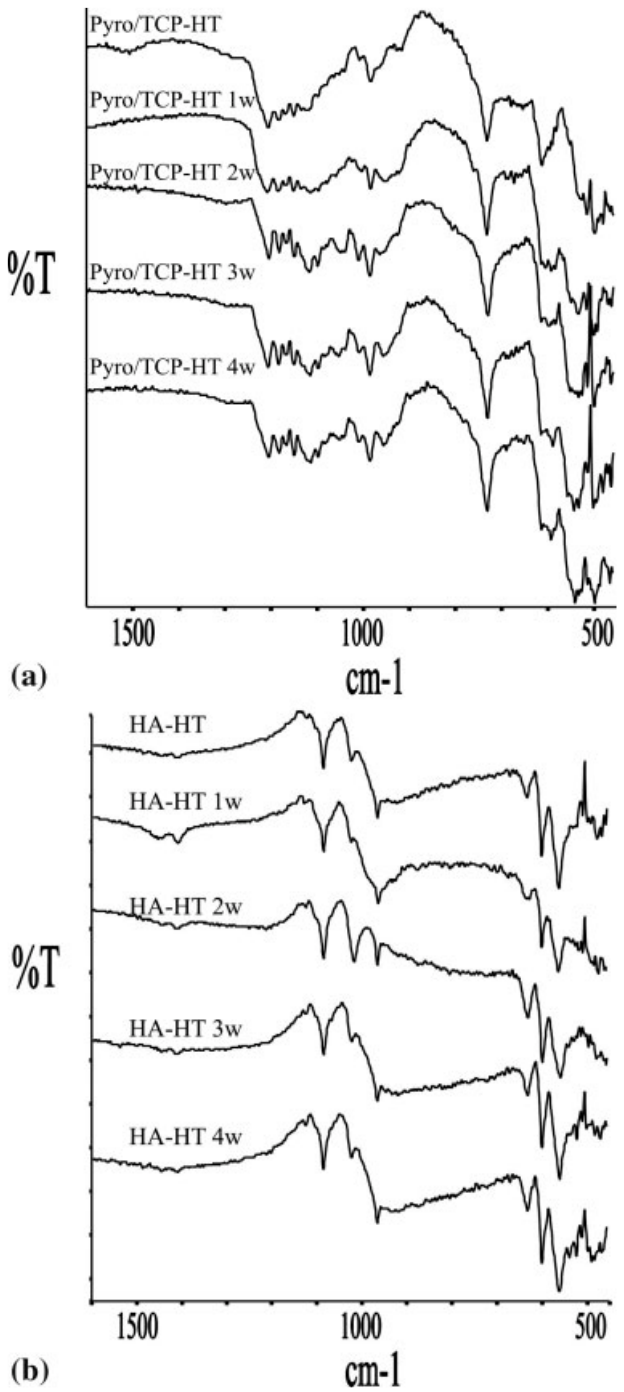

Figure 5. FTIR spectra of sputtered Ca-P coatings after incubation in SBF; (a) pyro/TCP coatings (b) HA coatings.

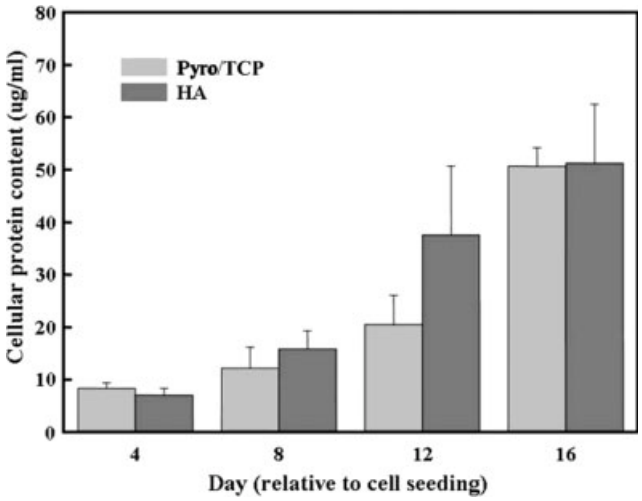

Figure 6. Protein content of the osteoblast-like cells on Pyro/TCP and HA coatings at the end of the various incubation times. Values represent mean ± SD.

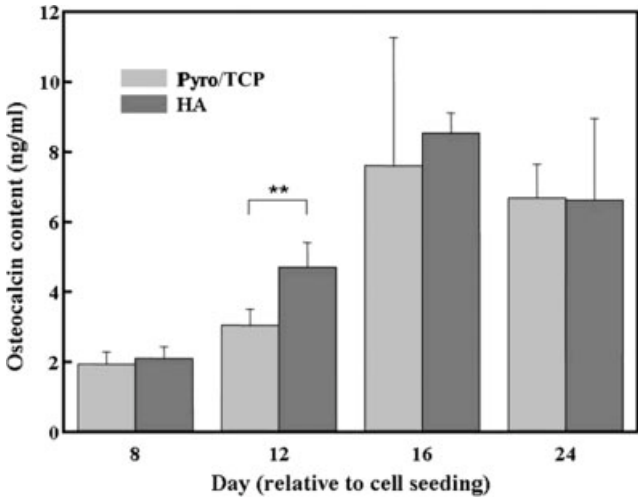

Figure 8. Osteocalcin expression of the osteoblast-like cells on Pyro/TCP and HA coatings at the end of the various incubation times. Values represent mean ± SD. ** indicates a significant difference ($p < 0.01$).

explained by the difference in activation energy for the crystallization of apatite compared to Pyro/TCP.[4] Further, this study demonstrated that IR-radiation is an excellent method to crystallize thin RF magnetron-sputtered Ca-P coatings.

The EDS measurements proved that the Ca/P ratio of the magnetron sputtered Pyro/TCP and HA coatings as used in this study were higher than the theoretical values, that is for Pyro/TCP 1.43 instead of 1.25 and for HA 1.97 instead of 1.67. It has been shown previously that the increase in Ca/P ratio of the Pyro/TCP and HA is mainly caused by the effect of preferential sputtering of calcium because of the possibility of the phosphorus ions being pumped away before reaching the substrate.[24] Further, sputtering deposition parameters, like power and Argon pressure, can affect the final Ca/P ratio of the sputtered coatings.[25]

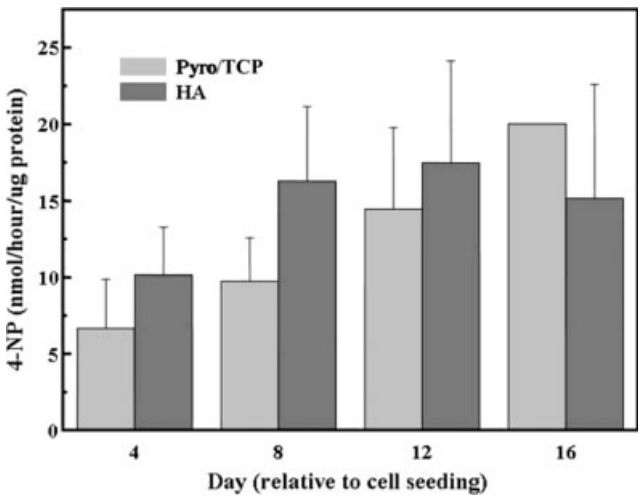

Figure 7. Alkaline phosphatase activity of the osteoblast-like cells on Pyro/TCP and HA coatings at the end of the various incubation times. Values represent mean ± SD.

Also the changes in Ca/P ratio of heat-treated Pyro/TCP coating after immersion in SBF indicated that the CaP phases are chemically instable, resulting in an increase of Ca/P ratio. On the other hand the Ca/P ratio of crystalline HA coating remained constant indicating stability of this CaP phase. The increase in Ca/P ratio of heat-treated Pyro/TCP is the result of a surface reaction of calcium pyrophosphate into a β-TCP phase.[26] It is claimed, that this kind of surface reactions benefits the osteogenic properties of the CaP coating.

A number of studies have addressed that the formation of directly bonded apatite is indicative for potential *in vivo* bioactivity.[27] In this study, no precipitation was observed on HA and Pyro/TCP coatings even after an incubation period of 4 weeks. This is likely because of the Ca and PO_4 concentrations of SBF solution used in the immersion experiment. Van der Wal et al.[28] indicated that the formation of a Ca-P precipitate on ceramic coatings only occurs in SBF_x, which is SBF with x times the human blood plasma Ca and PO_4 concentrations, with $x > 1.4$. Furthermore, Ca/P ratio, crystallinity, grain size of CaP coatings, and the presence of impurities in the coatings are important factors in the formation of CaP precipitation.

In the cell culture experiments, the proliferation of osteoblast-like cells was measured using protein analyses. Although this analysis does not measure intracellular protein exclusively, the amount of protein from other sources (e.g. extracellular matrix) will be limited because of the use of procedures (e.g. freeze and thaw cycles in water) with limited destructive effects on other protein sources than cells. The current study indicated an improved osteogenic effect of magnetron sputtered crystalline HA coatings compared to crystal-

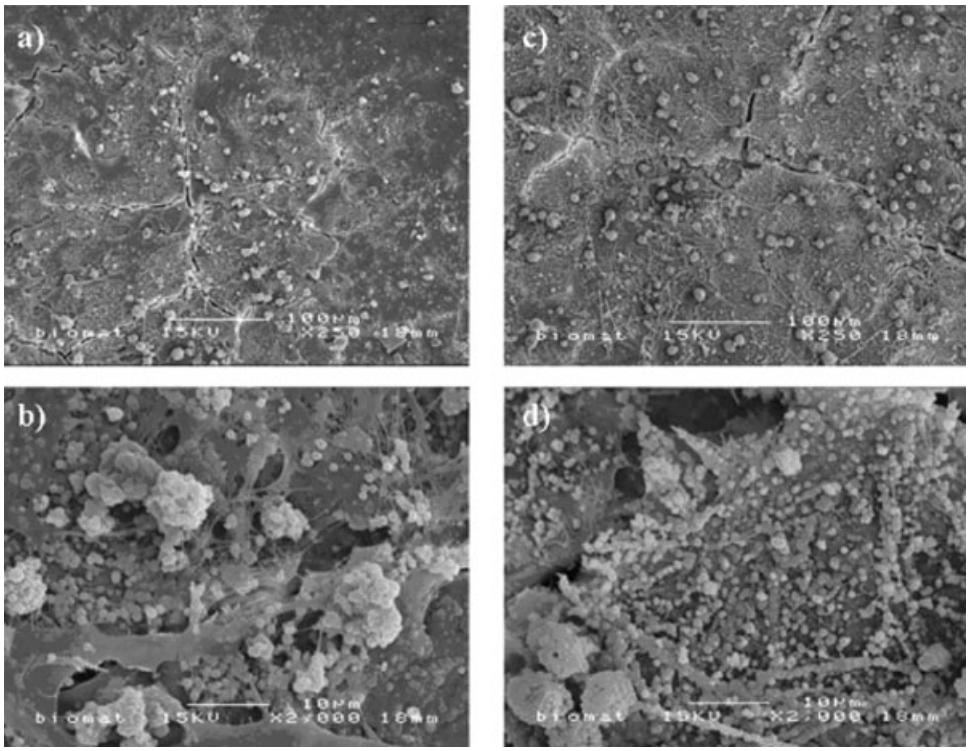

Figure 9. SEM pictures of osteoblast-like cells after 24 days on Pyro/TCP and HA coatings; (a, b) pyro/TCP surfaces (c, d) HA surfaces.

line Pyro/TCP coatings because the level of ALP and OC expression, which is supposed to reflect differences in the degree of differentiation of osteoblastic cells, started to increase earlier on the crystalline HA coatings. This observation most likely is related to the primary instability of Pyro/TCP coatings, as Pioletti et al. showed that dissolution of Ca-P coatings results in an increase of interfacial ions, which may cause apoptosis of osteogenic cells and cause damage to already formed bone.[29] Besides ions, also Ca-P particles can be released from the materials, which again have been shown to inhibit osteoblast function.[30] In this study, the Pyro/TCP coated film showed no dissolution in SBF by SEM observation. Consequently, the Pyro/TCP coatings were not enhancing cell differentiation and mineralization.

CONCLUSION

It can be concluded that RF magnetron sputtering can be successfully used to deposit Pyro/TCP and HA coatings on metal substrates, which can be transformed into crystalline phases using infrared heat-treatment. After immersion in SBF, heat-treated HA coatings were stable and showed no change in Ca/P ratio, whereas for Pyro/TCP coatings an increase in Ca/P ratio was observed. No CaP precipitation was observed on both Pyro/TCP and HA coatings after SBF immersion up to 4 weeks. The rat bone marrow derived osteoblast-like cells showed improved osteogenic response on HA coatings compared to Pyro/TCP coatings. As it is known that *in vitro* data cannot be directly extrapolated to the *in vivo* situation, further investigations are necessary to obtain conclusive evidence on the *in vivo* osteogenic capacity of Pyro/TCP coatings.

References

1. Schopper C, Moser D, Goriwoda W, Ziya-Ghazvini F, Spassova E, Lagogiannis G, Auterith A, Ewers R. The effect of three different calcium phosphate implant coatings on bone deposition and coating resorption: A long-term histological study in sheep. Clin Oral Implants Res 2005;16:357–368.
2. Klein CPAT, Wolke JGC, de Blieck-Hogervorst JMA, de Groot K. Features of calcium phosphate plasma-sprayed coatings: An in vitro study. J Biomed Mater Res 1994;28:909.
3. Yoshinari M, Ozeki K, Sumii T. Properties of hydroxyapatite-coated Ti-6Al-4V alloy produced by the ion-plating method. Bull Tokyo Dent Coll 1991;32:147–156.
4. Yanggang Yan, Wolke JGC, Yubao Li, Jansen JA. Preparation and characterization of RF magnetron sputtered calcium pyrophosphate coatings. J Biomed Mater Res A 2006;76:744–752.
5. Hayakawa T, Yoshinari M, Kiba H, Yamamoto H, Nemoto K, Jansen JA. Trabecular bone response to surface roughened and calcium phosphate (Ca-P) coated titanium implants. Biomaterials 2002;23:1025–1031.

6. Leeuwenburgh SCG, Wolke JGC, Schoonman J, Jansen JA. Influence of deposition parameters on chemical properties of calcium phosphate coatings prepared by using electrostatic spray deposition. J Biomed Mater Res A 2005;74:275–284.
7. Leeuwenburgh SCG, Wolke JGC, Schoonman J, Jansen JA. Influence of deposition parameters on morphological properties of biomedical calcium phosphate coatings prepared using electrostatic spray deposition. Thin Solid Films 2005;472:105–113.
8. Leeuwenburgh SCG, Wolke JGC, Schoonman J, Jansen JA. Influence of precursor solution parameters on chemical properties of calcium phosphate coatings prepared using Electrostatic Spray Deposition (ESD). Biomaterials 2004;25:641–649.
9. Wolke JGC, de Groot K, Jansen JA. In vivo dissolution behavior of various RF magnetron sputtered Ca-P coatings. J Biomed Mater Res 1998;39:524–530.
10. Yoshinari M, Hayakawa T, Wolke JGC, Nemoto K, Jansen JA. Influence of rapid heating with infrared radiation on RF magnetron-sputterd calcium phosphate coatings. J Biomed Mater Res 1997;37:60–67.
11. Kasuga T, Nogami M, Niiomi M. Preparation of bioactive calcium pyrophosphate glass-ceramics. J Mater Sci Lett 2001;20: 1249–1251.
12. Anderson C, Cape RDT, Crilly RG, Hodsman AB, Wokfe BMJ. Preliminary observations of a form of coherence therapy for osteoporosis. Calcif Tissue Int 1984;36:341–343.
13. Compston JE. The therapeutic use of bisphosphonates. BMJ 1994;17:711–715.
14. Yildirim OS, Aksakal B, Hanyaloglu SC, Erdogan F, Okur A. Hydroxyapatite dip coated and uncoated titanium poly-axial pedicle screws: An in vivo bovine model. Spine 2006;31:215–220.
15. Yonggang Yan, JGC Wolke, Yubao Li, Jansen JA. Subcutaneous evaluation of RF magnetron-sputtered calcium pyrophosphate and hydroxylapatite-coated Ti implants. J Biomed Mater Res A 2006;77:815–822.
16. Costa Cde A, Sena LA, Pinto M, Muller CA, Cavalcanti JH, Soares Gde A. In vivo characterization of titanium implants coated with synthetic hydroxyapatite by electrophoresis. Braz Dent J 2005;16:75–81.
17. Lee Jae Hyup, Ryu HS, Lee DS, Hong Kug Sun, Chang BS, Lee CK. Biomechanical and histomorphometric study on the bone-screw interface of bioactive ceramic-coated titanium screws. Biomaterials 2005;26:3249–3257.
18. Yuan H, van Blitterswijk CA, de Groot K, de Bruijn JD. A comparison of bone formation in biphasic calcium phosphate (BCP) and hydroxyapatite (HA) implanted in muscle and bone of dogs at different time periods. J Biomed Mater Res A 2006;78: 139–147.
19. Klein CPAT, de Groot K, Chen W, Li Y, Zhang X. Osseous substance formation induced in porous calcium phosphate ceramics in soft tissues. Biomaterials 1994;15:31–34.
20. LeGeros RZ, Lin S, Rohanizadeh R, Mijares D, LeGeros JP. Biphasic calcium phosphate bioceramics: Preparation, properties and applications. J Mater Sci: Mater Med 2003;14:201–209.
21. Schopper C, Ziya-Ghazvini F, Goriwoda W, Moser D, Wanschitz F, Spassova E, Lagogiannis G, Auterith A, Ewers R. HA/TCP compounding of a porous CaP biomaterial improves bone formation and scaffold degradation—A long-term histological study. J Biomed Mater Res B 2005;74:458–467.
22. Kokubo T, Ito S, Huang ZT, Hayashi T, Sakka S, Kitsugi T, Yamamuro T. Ca, P-rich layer formed on high-strength bioactive glass-ceramic A-W. J Biomed Mater Res 1990;24:331–343.
23. Maniatopoulos C, Sodek J, Melcher AH. 1988. Bone formation in vitro by stromal cells obtained from bone marrow of young adult rats. Cell Tissue Res 1988;63:171–176.
24. Yamashita K, Arashi T, Kitagaki K, Yamasa S, Umegaki T. Preparation of apatite thin films through rf-sputtering from calcium phosphate glasses. J. Am Ceram Soc 1994;77:2401–2407.
25. van der Wal E, Wolke JGC, Jansen JA, Vredenberg AM. Initial reactivity of RF magnetron sputtered calcium phosphate thin films in simulated body fluids. App Surf Sci 2005;246:183–192.
26. Yubao L, Klein CPAT, de Wijn J, van de Meer S, de Grooe K. Shape change and phase transition of needle-like non-stoichiometric apatite crystals. J Mater Sci: Mater Med 1994;5:263–264.
27. Ducheyne P, Qiu Q. Bioactive ceramics: The effect of surface reactivity on bone formation and bone cell function. Biomaterials 1999;20:2287–2303.
28. van der Wal E, Vredenberg AM, ter Brugge PJ, Wolke JGC, Jansen JA. The in vitro behavior of as-prepared and pre-immersed RF-sputtered calcium phosphate thin films in a rat bone marrow cell model. Biomaterials 2006;27:1333–1340.
29. Pioletti DP, Takei H, Lin T, van Landuyt P, Ma QJ, Kwon SY, Sung KLP. The effects of calcium phosphate cement particles on osteoblast functions. Biomaterials 2000;21:1103–1114.
30. Yuan H, Yang Z, de Bruijn JD, de Groot K, Zhang X. Material-dependent bone induction by calcium phosphate cement: A 2.5-year study in dog. Biomaterials 2001;22:2617–2623.